Hindawi Publishing Corporation
Advances in Condensed Matter Physics
Volume 2014, Article ID 627975, 6 pages
http://dx.doi.org/10.1155/2014/627975

Research Article

Magnetic Properties of Well-Aligned ZnO Nanorod Arrays Grown by a Simple Hydrothermal Reaction

Jiangni Yun, Rui Qu, Zhiyong Zhang, and Jun Li

School of Information Science and Technology, Northwest University, Xi'an 710127, China

Correspondence should be addressed to Jiangni Yun; niniyun@nwu.edu.cn

Received 8 November 2013; Revised 23 January 2014; Accepted 31 January 2014; Published 29 April 2014

Academic Editor: Xuan Luo

Well-aligned ZnO nanorod arrays with room temperature ferromagnetism were prepared on glass substrate through hydrothermal method. The as-prepared nanorod arrays were characterized by X-ray diffraction (XRD), scanning electron microscopy (SEM), energy dispersive spectroscopy (EDS), photoluminescence (PL) spectrum, and magnetization measurements. The XRD and SEM results indicated that the ZnO nanorods are with the wurtzite structure and exhibit preferential (002) orientation with *c*-axis perpendicular to the substrate surface. The PL results suggested that the possible defect in the as-prepared ZnO nanorod arrays might be V_{Zn}, O_i, or O_{Zn}. The first-principles calculations reveal that the room temperature ferromagnetism may result from the V_{Zn} defects present in the ZnO nanorod and the hybridization of the Zn 3d states with O 2p states is responsible for the half-metallic ferromagnetism in ZnO nanorod.

1. Introduction

Recently, one-dimensional (1D) ZnO nanorods have attracted great interest due to their tunable magnetic and opto-electronic properties [1–8]. Particularly, for the potential applications in the spin electronics, the investigation to grow well-aligned ZnO nanorod arrays with room temperature ferromagnetism has been an urgent task because it is a key process toward realizing nanoscale devices [9–11]. Synthesis methods, such as physical vapor deposition [12], chemical vapor deposition [13], and pulsed laser deposition [14], have been extensively used to obtain 1D well-aligned ZnO nanorod arrays. However, these vapor-phase processes fabrication techniques need vacuum condition, high energy consumption, sophisticated equipment, and rigid experimental conditions. Compared with the vapor-phase processes, the hydrothermal process is a low cost and environmentally friendly method, which is highly welcomed by numerous researchers [15–18].

In this study, well-aligned, single crystalline ZnO nanorod arrays with room temperature ferromagnetism and high packing density were achieved via a simple hydrothermal process. A possible origin of the ferromagnetism in the prepared ZnO nanorod arrays related to the intrinsic defect is proposed.

2. Experimental Details

The procedure of the ZnO nanorod arrays prepared under hydrothermal condition consists of two steps: (a) preparation of ZnO seed-layer and (b) growth of ZnO nanorod arrays. In the first step, a layer of ZnO seed crystal was deposited on the glass substrate via sol-gel method. In detail, equal molar Zn $(CH_3COO)_2$-$2H_2O$ and glycolic amide (0.35 mol/L) were solved in ethanol with stirring at 60°C for 12 h to yield a homogeneous solution. Subsequently, the precursor solution was dropped on the glass substrate, spinning at 3000 r/min for 30 s. Then the substrate was preheated in air at 80°C for 10 min. After that, the substrates were annealed at 500°C for 90 min in air to obtain a dense and transparent ZnO seed layer on the glass substrate by using an electronic furnace. In the second step, the glass substrate with a layer of ZnO seed crystal was placed into one autoclave filled with the precursor solutions of Zn $(CH_3COO)_2$-$2H_2O$ (0.04 M) and

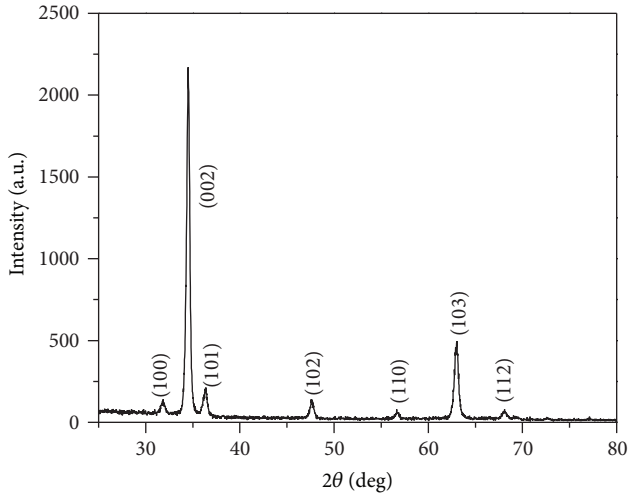

Figure 1: XRD pattern of the as-prepared ZnO nanorod arrays.

NaOH (0.08 M). After the autoclave is sealed safely, it is put into a bake oven at 120°C for 90 min. Finally, the glass substrate with white deposit is purged in deionized water for several times.

The obtained products are characterized by using X-ray diffraction (XRD, D/Max2550VB+/PC, Rigaku, Japan), scanning electron microscope (SEM, JSM-6390A, JEOL, Japan), photoluminescence spectrum (PL, FluoroMax-4p, HORIBA Jobin Yvon, USA), and a superconducting quantum interference device (MPMS-XL-7, Quantum Design, USA).

3. Results and Discussion

Figure 1 shows XRD pattern of the as-prepared sample. It is observed that all of the diffraction peaks can be well indexed to a wurtzite structure of ZnO. The strong and narrow diffraction peaks indicate that the material has a good crystallinity. In particular, the as-prepared sample exhibits preferential (0 0 2) orientation with *c*-axis perpendicular to the substrate surface.

Figures 2(a) and 2(b) depict the SEM images of the prepared ZnO nanorod arrays. The low-magnification SEM image in Figure 2(a) demonstrates that the nanorod array is uniform and densely packed. From the high-magnification image in Figure 2(b), it can be seen that the prepared ZnO nanorod array exhibits typical wurtzite structure and preferential (0 0 2) orientation with *c*-axis perpendicular to the substrate surface, which is reflected by the XRD pattern shown in Figure 1. Furthermore, energy dispersive spectroscopy (EDS) result indicates that the as-prepared ZnO nanorod array is only composed of Zn and O, and the atomic ratio of Zn and O is about 48.24 : 51.76. This suggests that the as-prepared nanorod arrays are nonstoichiometric and some defects may exist in the as-prepared nanorod arrays.

Figure 3 shows the room temperature PL spectra of the as-prepared ZnO nanorod arrays. A strong UV emission peak at 373 nm and three relatively weak and broad visible emissions centered at 425, 511, and 590 nm, respectively, can

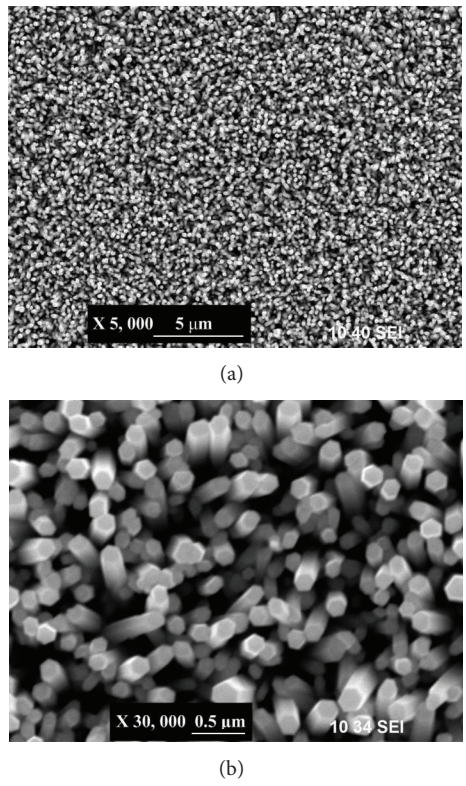

Figure 2: SEM images of ZnO nanorod arrays. (a) Large-scale and low magnification and (b) high magnification.

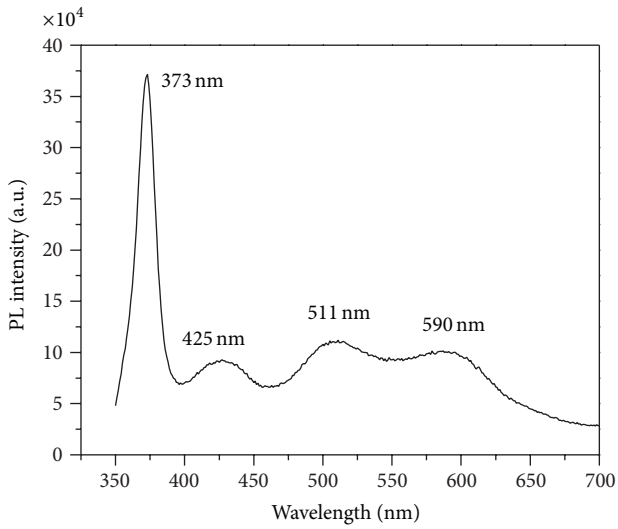

Figure 3: Room temperature PL spectra of the ZnO nanorod arrays.

be observed. The UV emission band is usually attributed to the near-band edge emission of the wide band gap of ZnO due to the annihilation of excitons [8, 19–21]. The visible emission is the most commonly observed and is often attributed to the defect emission [22–27]. It is known that different defects may cause different electronic structures, which will be reflected on the corresponding optical properties observed in experiments. On the other hand, the electronic structure

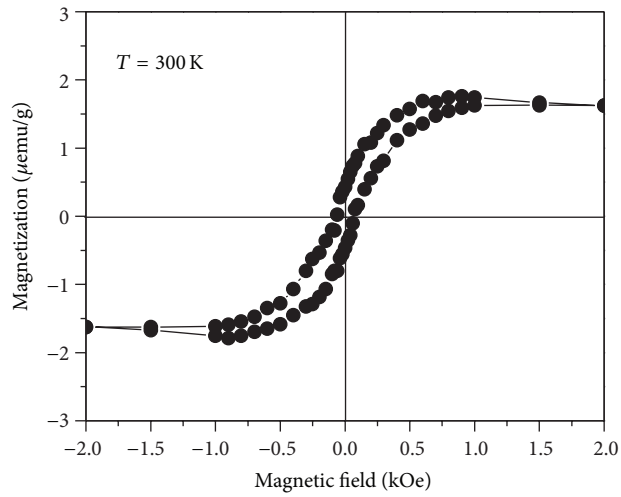

Figure 4: Magnetization hysteresis loops of ZnO nanorod arrays at 300 K.

of the defects can be predicted unambiguously from density functional calculations. Hence, combining the experimental observations with theoretical results may identify different defects such as oxygen vacancy (V_O), antisite oxygen (O_{Zn}), zinc vacancy (V_{Zn}), zinc interstitial (Zn_i), and oxygen interstitial (O_i) in ZnO. Theoretically, Xu et al. and Sun et al. [26, 27] calculated the electronic structure of native point defects in ZnO. Based on their results, the energy interval between the bottom of the conduction band (CB) and V_{Zn} level (3.06 eV) is approximately consistent with the energy of the blue-purple emission (425 nm, 2.92 eV) observed in our experiment. The energy interval from the bottom of the CB to the O_{Zn} level (2.38 eV) is consistent with the energy of the green emission (511 nm, 2.43 eV). The energy interval between the bottom of the CB and O_i level (2.28 eV) approximately conforms to the yellow emission (590 nm, 2.10 eV). By analysis of the experimental phenomena and the calculation of the defect levels in ZnO, we suggest that the blue emission centered at 425 nm is attributed to V_{Zn} [26, 27], the green emission centered at 511 nm originates from O_{Zn} [26, 27], and the yellow emission centered at 590 nm is related to O_i [26]. Therefore the PL results reveal that the possible defect in the as-prepared ZnO nanorod arrays might be V_{Zn}, O_i, or O_{Zn}.

Figure 4 shows the magnetization as a function of the applied field at 300 K for the as-prepared ZnO nanorod arrays. The diamagnetic contribution from the glass substrate has been subtracted from the raw data. It is interesting that the ZnO nanorod arrays exhibit room temperature ferromagnetism. The saturation magnetization M_s and remanent magnetization M_r are about 1.7×10^{-3} and 4.33×10^{-4} emu/g, respectively. The coercivity H_c is about 60 Oe. As we know, neither doping nor evidence of secondary phase exit in the as-prepared ZnO nanorod arrays; the observed room temperature ferromagnetism in the as-prepared ZnO nanorod arrays probably results from the intrinsic defect.

In order to provide more insight into this issue, we employed first-principles calculation [28] on the electronic structure and magnetic properties for the ZnO nanorod. Since the PL study results reveal that the possible defect in the as-prepared ZnO nanorod arrays might be V_{Zn}, O_i, or O_{Zn}, thus, in the present calculations, the ZnO nanorods with V_{Zn}, O_i, or O_{Zn} defect are investigated. The wurtzite supercell containing 96 atoms is used for calculation. For the ZnO nanorod with V_{Zn} or O_{Zn} defect, there are three inequivalent defect positions, which are denoted as V_{Zn1}–V_{Zn3} and O_{Zn1}–O_{Zn3}, as shown in Figures 5(a) and 5(b). However, there are two inequivalent O_i defect positions, which are denoted as O_{i1} and O_{i2} as shown in Figure 5(c). The formation energy of V_{Zn} at V_{Zn2} site is about 0.12 and 0.38 eV smaller than that at the V_{Zn1} and V_{Zn3} sites, respectively, and, thus, V_{Zn2} is the most stable site for V_{Zn} defect. Similar to V_{Zn}, O_{Zn} also prefers at the O_{Zn2} site. While for the O_i defect, it prefers at the O_{i1} site. Therefore, the magnetic properties of ZnO nanorod with V_{Zn}, O_{Zn}, and O_i are calculated based on the V_{Zn2}, O_{Zn2}, and O_{i1} geometries, respectively.

The calculated densities of states (DOSs) for the ZnO nanorod with V_{Zn}, O_i, or O_{Zn} defect are shown in Figure 6. It is clear that the spin-up and spin-down DOSs of pure ZnO nanorod are completely symmetrical, indicating that the pure ZnO nanorod is nonmagnetic. Similarly, the ZnO nanorod with O_i or O_{Zn} defect also exhibits nonmagnetic properties. As for the ZnO nanorod with V_{Zn} defect, however, a strong spin splitting phenomenon is observed. The Fermi level passes through the band gap in the spin-down DOS and an energy gap of about 1.47 eV exists in the spin-up DOS. This demonstrates that the ZnO nanorod with V_{Zn} behaves as half-metallic.

By analysis of the partial densities of states (PDOSs) in Figure 7, it can be found that the metallic spin-down DOS near the Fermi level is mainly composed of Zn 3d and O 2p states. In particular, O 2p states make significant contribution to the magnetic moment. This suggests that the appearance of the half-metallic ferromagnetism in ZnO nanorod with V_{Zn} originates from the hybridization of the Zn 3d states with O 2p states.

4. Conclusions

In conclusion, ZnO nanorod arrays with room temperature ferromagnetism were prepared on glass substrate through hydrothermal method. The as-prepared sample shows preferential (0 0 2) orientation with *c*-axis perpendicular to the substrate surface. The room temperature PL measurements exhibit a prominent UV peak at about 373 nm which is attributed to the annihilation of excitons. Three relatively weak and broad visible emissions resulting from the defects can also be observed in the PL spectrum. By analysis of the calculated electronic structure of the ZnO nanorod with defects, we can get the conclusion that the V_{Zn} defects present in the ZnO nanorods are responsible for the room temperature ferromagnetism.

Conflict of Interests

The authors declare that there is no conflict of interests regarding the publication of this paper.

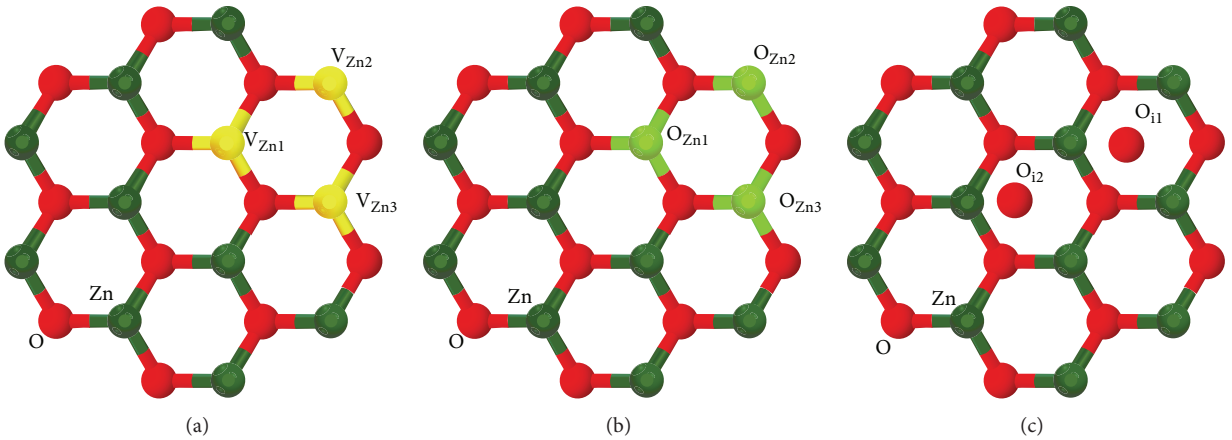

FIGURE 5: The structure of ZnO nanorods (a) with V_{Zn}, (b) with O_i, and (c) with O_{Zn} defect.

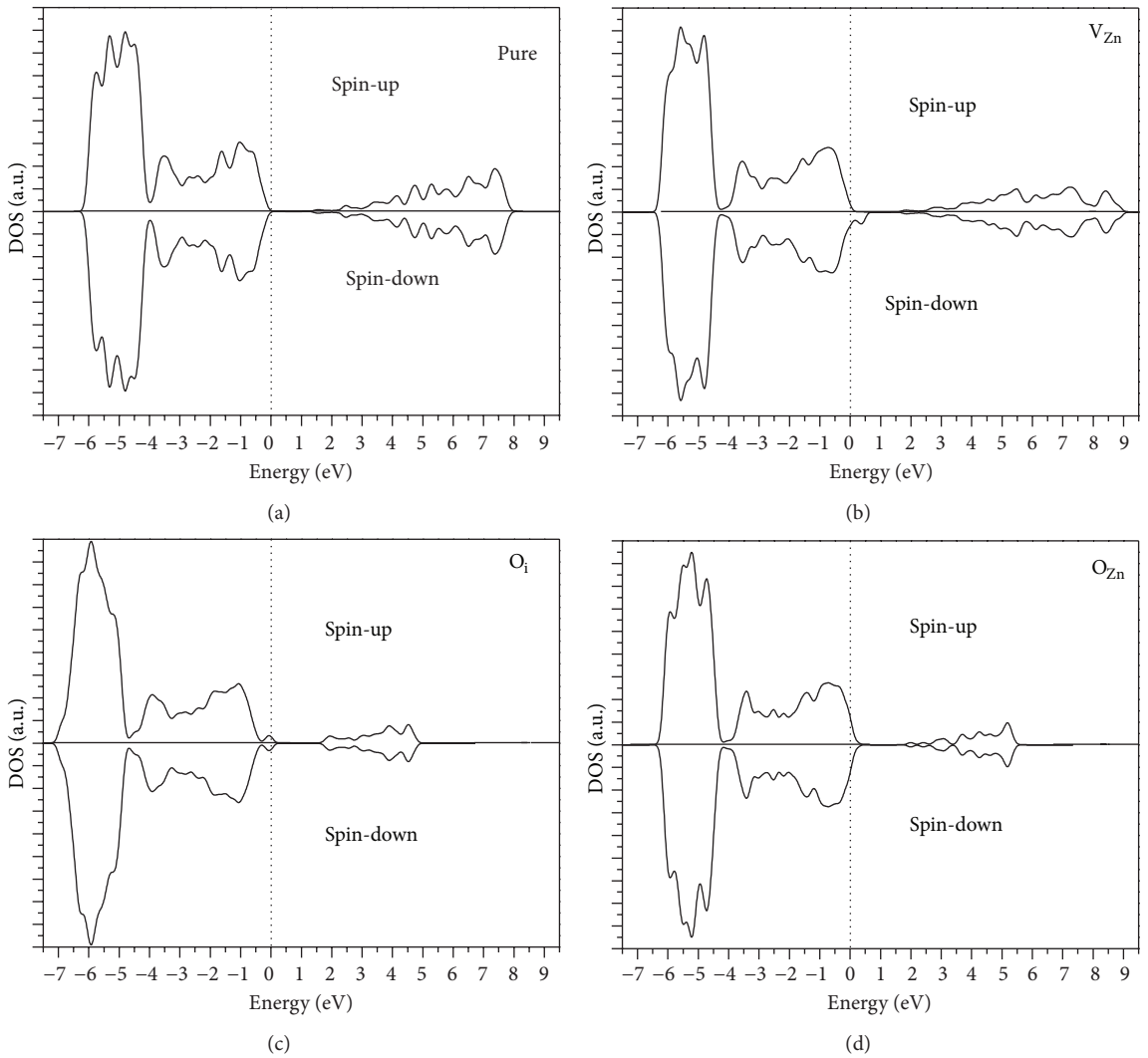

FIGURE 6: Calculated DOSs for ZnO nanorod. The Fermi level is set to zero on the energy scale, which will be adopted below unless otherwise stated.

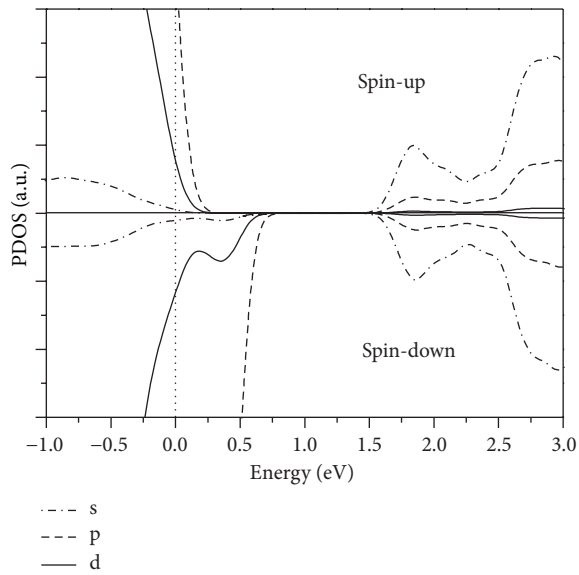

FIGURE 7: Calculated PDOS for ZnO nanorod with V_{Zn} defect.

Acknowledgments

This work is supported by the Natural Science Basic Research Plan in Shaanxi Province of China (Program nos. 2011JQ8034 and 2013KJXX-24), the Open Foundation of Key Laboratory of Photoelectronic Technology of Shaanxi Province (Grant no. ZS11009), the Science Foundation of Northwest University (nos. 10NW08 and PR10069), and the NWU Graduate Innovation and Creativity Funds (09YZZ64). The authors are also thankful for the support of the Scientific Research Program funded by the Shaanxi Provincial Education Department (Program no. 11JK0831).

References

[1] W. Wu, G. Hu, S. Cui, Y. Zhou, and H. Wu, "Epitaxy of vertical ZnO nanorod arrays on highly (001)-oriented ZnO seed monolayer by a hydrothermal route," *Crystal Growth and Design*, vol. 8, no. 11, pp. 4014–4020, 2008.

[2] J. T. Chen, J. Wang, R. F. Zhuo et al., "The effect of Al doping on the morphology and optical property of ZnO nanostructures prepared by hydrothermal process," *Applied Surface Science*, vol. 255, no. 7, pp. 3959–3964, 2009.

[3] Z. Y. Wang, B. Huang, X. Qin et al., "Growth of high transmittance vertical aligned ZnO nanorod arrays with polyvinyl alcohol by hydrothermal method," *Materials Letters*, vol. 63, no. 1, pp. 130–132, 2009.

[4] T. G. You, J. Yan, Z. Zhang et al., "Fabrication and optical properties of needle-like ZnO array by a simple hydrothermal process," *Materials Letters*, vol. 66, no. 1, pp. 246–249, 2011.

[5] S. Ilican, "Effect of Na doping on the microstructures and optical properties of ZnO nanorods," *Journal of Alloys and Compounds*, vol. 553, pp. 225–232, 2013.

[6] M. Guo, P. Diao, and S. Cai, "Hydrothermal growth of well-aligned ZnO nanorod arrays: dependence of morphology and alignment ordering upon preparing conditions," *Journal of Solid State Chemistry*, vol. 178, no. 6, pp. 1864–1873, 2005.

[7] Z. Li, X. Huang, J. Liu, Y. Li, X. Ji, and G. Li, "Growth and comparison of different morphologic ZnO nanorod arrays by a simple aqueous solution route," *Materials Letters*, vol. 61, no. 22, pp. 4362–4365, 2007.

[8] M. H. Huang, S. Mao, H. Feick et al., "Room-temperature ultraviolet nanowire nanolasers," *Science*, vol. 292, no. 5523, pp. 1897–1899, 2001.

[9] Y. Lee, Y. Zhang, S. L. G. Ng, F. C. Kartawidjaja, and J. Wang, "Hydrothermal growth of vertical ZnO nanorods," *Journal of the American Ceramic Society*, vol. 92, no. 9, pp. 1940–1945, 2009.

[10] H. L. Yan, X. L. Zhong, J. B. Wang et al., "Cathodoluminescence and room temperature ferromagnetism of Mn-doped ZnO nanorod arrays grown by chemical vapor deposition," *Applied Physics Letters*, vol. 90, no. 8, Article ID 082503, 2007.

[11] A. B. Djuriić, A. M. C. Ng, and X. Y. Chen, "ZnO nanostructures for optoelectronics: material properties and device applications," *Progress in Quantum Electronics*, vol. 34, no. 4, pp. 191–259, 2010.

[12] E. Oh, S.-H. Jung, K.-H. Lee, S.-H. Jeong, S. Yu, and S. J. Rhee, "Vertically aligned Fe-doped ZnO nanorod arrays by ultrasonic irradiation and their photoluminescence properties," *Materials Letters*, vol. 62, no. 19, pp. 3456–3458, 2008.

[13] J. Wu, S. Liu, and M. Yang, "Room-temperature ferromagnetism in well-aligned $Zn_{1-x}Co_xO$ nanorods," *Applied Physics Letters*, vol. 85, no. 6, pp. 1027–1029, 2004.

[14] J. J. Chen, M. H. Yu, W. L. Zhou, K. Sun, and L. M. Wang, "Room-temperature ferromagnetic Co-doped ZnO nanoneedle array prepared by pulsed laser deposition," *Applied Physics Letters*, vol. 87, no. 17, p. 173119, 2005.

[15] J. Xu, Y. P. Chen, D. Y. Chen, and J. N. Shen, "Hydrothermal synthesis and gas sensing characters of ZnO nanorods," *Sensors and Actuators B: Chemical*, vol. 113, no. 1, pp. 526–531, 2006.

[16] S. Kumar, Y. J. Kim, B. H. Koo et al., "Room temperature ferromagnetism in chemically synthesized ZnO rods," *Materials Letters*, vol. 63, no. 2, pp. 194–196, 2009.

[17] L. Z. Pei, H. S. Zhao, W. Tan et al., "Hydrothermal oxidization preparation of ZnO nanorods on zinc substrate," *Physica E: Low-Dimensional Systems and Nanostructures*, vol. 42, no. 5, pp. 1333–1337, 2010.

[18] A. Aravind, M. K. Jayaraj, M. Kumar, and R. Chandra, "Optical and magnetic properties of copper doped ZnO nanorods prepared by hydrothermal method," *Journal of Materials Science: Materials in Electronics*, vol. 24, no. 1, pp. 106–112, 2013.

[19] H. G. Kim, D. W. Hwang, and J. S. Lee, "An undoped, single-phase oxide photocatalyst working under visible light," *Journal of the American Chemical Society*, vol. 126, no. 29, pp. 8912–8913, 2004.

[20] R. Elilarassi and G. Chandrasekaran, "Structural, optical and magnetic properties of nanoparticles of ZnO:Ni—DMS prepared by sol-gel method," *Materials Chemistry and Physics*, vol. 123, no. 2-3, pp. 450–455, 2010.

[21] K. H. Tam, C. K. Cheung, Y. H. Leung et al., "Defects in ZnO Nanorods Prepared by a Hydrothermal Method," *The Journal of Physical Chemistry B*, vol. 110, no. 42, pp. 20865–20871, 2006.

[22] F. Ahmed, S. Kumar, N. Arshi, M. S. Anwar, B. H. Koo, and C. G. Lee, "Defect induced room temperature ferromagnetism in well-aligned ZnO nanorods grown on Si (100) substrate," *Thin Solid Films*, vol. 519, no. 23, pp. 8199–8202, 2011.

[23] Q. X. Zhao, P. Klason, and M. Willander, "Deep-level emissions influenced by O and Zn implantations in ZnO," *Applied Physics Letters*, vol. 87, no. 21, p. 211912, 2005.

[24] A. F. Kohan, G. Ceder, D. Morgan, and C. G. van de Walle, "First-principles study of native point defects in ZnO," *Physical Review B—Condensed Matter and Materials Physics*, vol. 61, no. 22, pp. 15019–15027, 2000.

[25] A. B. Djurišić and Y. H. Leung, "Optical properties of ZnO nanostructures," *Small*, vol. 2, no. 8-9, pp. 944–961, 2006.

[26] P. S. Xu, Y. M. Sun, C. S. Shi, F. Q. Xu, and H. B. Pan, "The electronic structure and spectral properties of ZnO and its defects," *Nuclear Instruments and Methods in Physics Research B: Beam Interactions with Materials and Atoms*, vol. 199, pp. 286–290, 2003.

[27] Y. M. Sun, *FP-LMTO study on the electronic structure of ZnO and its defects [Ph.D. dissertation]*, University of Science and Technology of China, 2000.

[28] M. D. Segall, P. J. D. Lindan, M. J. Probert et al., "First-principles simulation: ideas, illustrations and the CASTEP code," *Journal of Physics Condensed Matter*, vol. 14, no. 11, pp. 2717–2744, 2002.